Optical properties of vacuum evaporated $Cd_xSn_{1-x}Se$ polycrystalline thin films: influence of composition and thickness

D. Pathinettam Padiyan[a,*], A. Marikani[b], K.R. Murali[c]

[a]*Department of Physics, Manonmaniam Sundaranar University, Tirunelveli-627 012, India*
[b]*Mepco Schlenk Engineering College, Virudhunagar-Dt.-626 005, Tamil Nadu, India*
[c]*Central Electrochemical Research Institute, Karaikudi-630 006, Tamil Nadu, India*

Abstract

Polycrystalline $Cd_xSn_{1-x}Se$ material is synthesized by melt growth technique for various x values and thin films are prepared by vacuum evaporation technique. Optical transmittance measurements have been made on thin films of $Cd_xSn_{1-x}Se$, with $x = 0, 0.3, 0.75$ and 1 for various thicknesses. The studies reveal that these thin films have a direct allowed band gap energy and the indirect band gap energy is improbable. The band gap energy increases with decrease in thickness in all the compositions and it is attributed to the quantum size effect.
© 2004 Elsevier B.V. All rights reserved.

1. Introduction

Metal selenide thin films offer a range of optical band gap energies suitable for various optical and optoelectronic applications. Thin films of tin selenide have great potential applications, such as memory switching devices [1]. CdSe thin films have found applications in solar cells, thin film transistors [2,3] and gamma-ray detectors [4]. CdSe and SnSe have been studied in the form of both thin films and single crystals [5–8]. CdSe is a narrow band semiconductor and its optical band gap is 1.74 eV [9], whereas SnSe have the band gap energy of 0.9 eV [10]. This difference in energy gap lies in the optical absorption spectrum of solar radiation and hence the study of the optical properties of $Cd_xSn_{1-x}Se$ with $x = 0, 0.3, 0.75$ and 1 thin films is carried out. No study has been

*Corresponding author. Fax: +91 462 232 2973.
E-mail addresses: dppadiyan@rediffmail.com
(D.P. Padiyan), amari@mepcoeng.ac.in (A. Marikani).

reported in the literature for $Cd_xSn_{1-x}Se$ solid solutions either in the form of thin films or single crystals. This paper characterizes the band gap energy and optical absorption coefficient of SnSe, $Cd_{0.3}Sn_{0.7}Se$, $Cd_{0.75}Sn_{0.25}Se$ and CdSe thin films prepared by vacuum deposition technique.

2. Experimental methods

The bulk $Cd_xSn_{1-x}Se$ materials with $x = 0, 0.3$ and 0.75 were synthesized in a quartz ampoule by mixing cadmium metal, tin and selenium (Aldrich, 99.99% pure) powders in their stoichiometric ratio by melt growth technique. The synthesized compound was analyzed by X-ray diffraction technique for their homogeneity and crystalline nature. The composition analysis of the synthesized powder materials was carried out using atomic absorption spectrophotometer.

The synthesized $Cd_xSn_{1-x}Se$ materials with $x = 0, 0.3$ and 0.75 and commercially available CdSe powder sample (Aldrich, 99.99% pure) were used to deposit thin films using Hind Hivac Vacuum Coating unit (model-12-A4) at different substrate temperatures and thicknesses. The powder materials were kept in a molybdenum boat during evaporation and the resistive evaporation technique was used to prepare thin films. The X-ray powder diffraction patterns for the synthesized $Cd_xSn_{1-x}Se$ with $x = 0, 0.3$ and 0.75 powder materials and CdSe powder material and thin films were recorded in JEOL JDX 8030 X-ray diffractometer using Cu Kα radiation at room temperature. The X-ray photoelectron spectroscopy (XPS) spectra were recorded for $Cd_xSn_{1-x}Se$ thin films in an ESCALAB MK II spectrometer (VG Scientific Ltd., UK) using Mg Kα radiation of energy 1253.6 eV. The optical transmission spectrum was recorded using a HITACHI model V-3400 UV-Vis-NIR spectrophotometer in the region 400–2000 nm. All the measurements were carried out at room temperature for normal incidence mode. The transmittance of the thin films was measured relative to that of an identical uncoated substrate. The estimated measurement error including the instrumental error in transmittance is less than 1%. Thin film

uniformity was checked by measuring the transmission curves at different areas of the film.

3. Results and discussion

3.1. Structure and composition

The X-ray powder diffraction data recorded for $Cd_xSn_{1-x}Se$ powder materials with $x = 0, 0.3, 0.75$ and 1 reveal that these powder materials are polycrystalline in nature. The XRD peaks are indexed with the help of the software DICVOL91 [11,12] and Hull and Davey chart [13]. The lattice parameters are evaluated using the indexed *hkl* values and the measured 2θ values using the software UNITCELL [14]. The refined cell parameters for all the materials are given in Table 1. CdSe powder material shows that it crystallizes in hexagonal crystal system, whereas SnSe, $Cd_{0.3}Sn_{0.7}Se$ and $Cd_{0.75}Sn_{0.25}Se$ powder materials show that they crystallize in orthorhombic crystal system as reported [15].

The XRD patterns recorded for the $Cd_xSn_{1-x}Se$ thin films with $x = 0, 0.3, 0.75$ and 1 are found to be polycrystalline in nature and their crystallinity increases with annealing. The XRD data recorded agrees well with the standard one. The composition of $Cd_xSn_{1-x}Se$ thin films with $x = 0.3, 0.75$ and 1 is found to be rich in selenium (1–3%) and cadmium deficient and is displayed in Table 2. The SnSe thin film is found to be selenium deficient.

3.2. Optical band gap energy

The optical absorption coefficient α is determined using the relation:

$$\alpha = \frac{2.303}{t}\log_{10}\left(\frac{1}{T}\right), \tag{1}$$

where t is the thickness of the film and T is the transmittance. The relation [16] between the photon energy and the optical absorption coefficient is

$$\alpha h\nu = A(h\nu - E_g \pm E_p)^x, \tag{2}$$

where E_g is the energy gap, E_p is the energy of the absorbed $(+)$ or emitted $(-)$ phonon energy. For

Table 1
Unit cell parameters for $Cd_xSn_{1-x}Se$ with $x = 0, 0.3, 0.75$ and 1 powder material

Sl.No	Composition	Crystal system	Cell constants		
			a (Å)	b (Å)	c (Å)
1	0	Orthorhombic	11.37(5)	4.44(2)	4.02(2)
2	0.3	Orthorhombic	12.11(2)	4.751(7)	3.79(2)
3	0.75	Orthorhombic	12.57(5)	4.19(3)	3.91(1)
4	1.0	Hexagonal	4.307(3)		7.03(1)

Table 2
Composition of the $Cd_xSn_{1-x}Se$ thin films with $x = 0, 0.3, 0.75$ and 1

Thin film sample	Composition of the film (at%)			Ratio relative to Se	
	Cadmium	Tin	Selenium	Cd	Sn
SnSe	—	50.3	49.7	—	1.012
$Cd_{0.3}Sn_{0.7}Se$	13.2	34.0	52.8	0.250	0.644
$Cd_{0.75}Sn_{0.25}Se$	35.1	13.0	51.9	0.676	0.250
CdSe	49.0	—	51.0	0.961	—

indirect allowed transition, $x = 2$ and 3 for indirect forbidden transition. The emission and absorption of a phonon in a room temperature transition will contribute some energy to the absorption. In a direct transition ($E_p = 0$), x is equal to 0.5 and 1.5 for allowed and forbidden transitions, respectively.

3.2.1. SnSe thin films

The optical transmission spectra of SnSe thin films of thickness $0.2\,\mu m$, as prepared and annealed in air at $300\,°C$ for $2\,h$, are shown in Fig. 1. The maximum transmittance value is shifted to the higher wavelengths on annealing due to increase in grain size. It is also observed that the optical transmittance decreases on annealing. A plot of $(\alpha h v)^2$ versus $h v$ for the as prepared and annealed tin selenide thin films is shown in Fig. 2. The plot is linear in the strong absorption near the fundamental absorption edge. The optical transmittance decreases on annealing. Since the absorption coefficient is very large and it is measured at room temperature, the presence of the indirect band gap as in the case of the bulk sample is improbable [16,17]. It is reasonable to consider that the absorption of SnSe evaporated
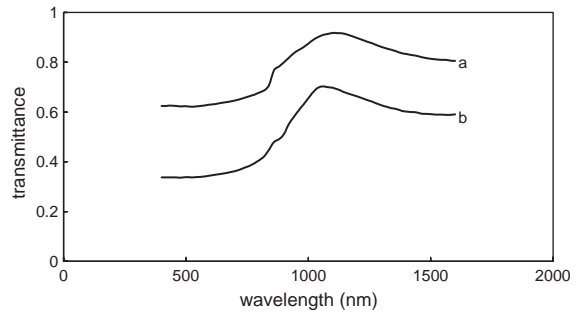

Fig. 1. A plot of transmittance against wavelength for (a) as prepared and (b) annealed at $300\,°C$ for SnSe thin films of thickness $0.2\,\mu m$ prepared at a substrate temperature of $150\,°C$.

thin films is due to an allowed direct transition from the top of the valence band to the bottom of the conduction band at the centre of the Brillouin zone.

The optical band gap energy obtained is $1.26(4)\,eV$ for the as prepared film and $1.23(3)\,eV$ for the film annealed at $300\,°C$. It is in good agreement with the reported value for SnSe thin films prepared by other methods [18,19]. The observed decrease in the band gap energy and
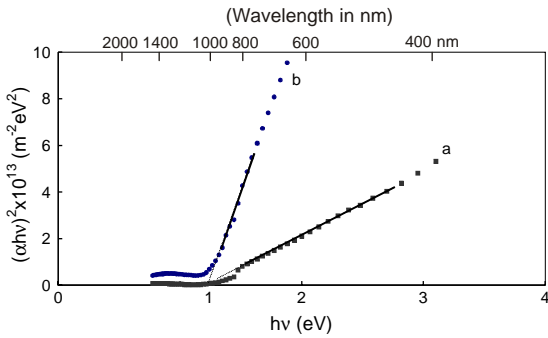
Fig. 2. A plot of $(\alpha h v)^2$ versus hv for (a) as prepared SnSe and (b) annealed at 300 °C SnSe thin films.

optical transmission can be related to the improvement in the crystallinity in annealed films [20].

A similar decrease in optical transmission spectra of the annealed films was observed by Nair et al. [21] for their cadmium selenide thin films prepared by chemical bath deposition. In SnSe$_2$ thin films a decrease in band gap values between the as deposited and the films annealed at 473 K was observed by Bhatt et al. [22]. The decrease in band gap energy of chemically deposited CdS thin film from 2.6 to 2.3 eV when annealed at 450 °C has been reported by George et al. [23].

According to Slater [24], in the case of polycrystalline films the intergrain barrier height increases due to change in the grain size. Slater's formula given by Damodara Das and Jagadeesh [25] for the barrier height is

$$E = \frac{N_o e^2}{4\varepsilon_r \varepsilon_o}\left(x - \frac{nD}{N_o}\right)^2, \qquad (3)$$

where e is the electronic charge, ε_r is the dielectric constant of the material, $\varepsilon_o = 8.854 \times 10^{-12}$ F/m, N_o is the density of charge carriers in the barrier, x is the thickness of the barrier, D is the dimension of the crystallites and n is the density of the electron–hole pairs created. The effect of these generated charge carriers is to reduce the barrier thickness and height by a constant factor (if n is constant) at a given temperature. It is clear from the above expression that the barrier height decreases as the crystallite size D increases. Thus

annealing results in an increase of grain size in the films, reducing the band gap.

3.2.2. CdSe thin films

The optical transmission spectra of the CdSe thin films prepared at room temperature for various thicknesses is shown in Fig. 3. A shift in the absorption maxima to the higher wavelength range is noticed for increase in thickness. The optical transmission of the film is above 80% for wavelengths greater than 590, 690, and 740 nm, respectively for 0.343, 0.403, and 0.497 μm thick films. This feature illustrates the good quality of CdSe thin films deposition by vacuum evaporation technique.

The plot of $(\alpha h v)^2$ versus hv for different thicknesses is shown in Fig. 4 for cadmium selenide thin films prepared at room temperature. For the films having thicknesses 0.343 and 0.403 μm, two linear regions are noticed whereas for the film of thickness 0.497 μm, only one straight line portion is identified. The band gap energies obtained for the film of thickness 0.343 μm are 1.79(4) and 1.98(1) eV and for the film of thickness 0.403 μm are 1.75(2) and 1.99(3) eV and for the film of thickness 0.497 μm is 1.73(2) eV. Similarly, two different band gap energies ranging from 1.67 to 1.74 eV and 1.71 to 2.09 eV have been reported by Shaalan and Müller [26] for CdSe thin films prepared by thermal evaporation technique having different thicknesses. Thutupalli and Tomlin [27] observed two
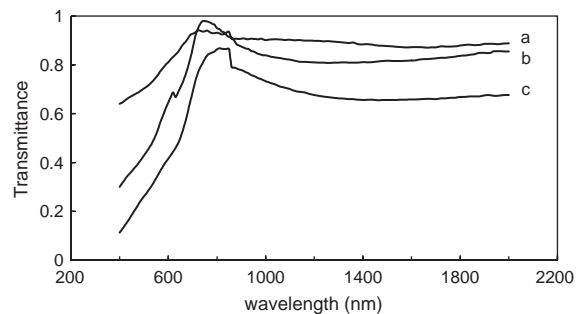

Fig. 3. Transmittance spectra of CdSe thin films prepared at room temperature and of thicknesses (a) 0.343 μm, (b) 0.403 μm and (c) 0.497 μm.
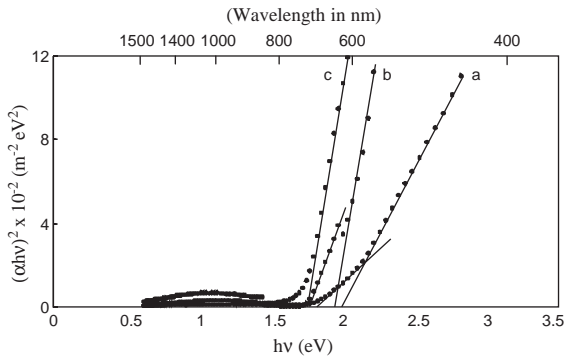
Fig. 4. A plot of $(\alpha h\nu)^2$ versus $h\nu$ for CdSe thin films prepared at room temperature and of thicknesses (a) 0.343 μm, (b) 0.403 μm and (c) 0.497 μm.

Fig. 5. Transmittance spectra of $Cd_{0.3}Sn_{0.7}Se$ thin films prepared at room temperature and of thicknesses (a) 0.225 μm, (b) 0.276 μm, (c) 0.3 μm and (d) 0.683 μm.

Fig. 6. A plot of $(\alpha h\nu)^2$ versus $h\nu$ for $Cd_{0.3}Sn_{0.7}Se$ thin films prepared at room temperature and of thicknesses (a) 0.225 μm, (b) 0.276 μm, (c) 0.3 μm and (d) 0.683 μm.

direct band gap energy values of 1.746 and 2.146 eV for their CdSe film prepared at a substrate temperature of 300 °C.

The two direct transitions can be attributed to spin–orbit splitting of the valence band that is in agreement with the findings of Cardona et al. [28] and Thutupalli and Tomlin [27]. These splittings are also noticed in the transmittance spectra of CdSe thin films at 590 and 620 nm for film of thicknesses of 0.343 and 0.403 μm, respectively as a small hump. But no such splitting could be detected for CdSe films having thickness 0.497 μm and for the films prepared at the substrate temperatures of 373 and 473 K. Two different E_g values are expected, if additional absorption processes cause the tail at the absorption edge, because of transitions from the higher valence level. A similar effect should occur when a transition from the lower of the split valence levels sets in. The spin–orbit splitting of the valence band for CdSe thin film sample of thickness 0.343 μm prepared at room temperature is 0.19 eV and another thin film sample of thickness 0.403 μm is 0.24 eV.

3.2.3. Mixed thin films

The optical transmission spectra of $Cd_{0.3}Sn_{0.7}Se$ thin film samples are shown in Fig. 5. A plot of $(\alpha h\nu)^2$ versus $h\nu$ for $Cd_{0.3}Sn_{0.7}Se$ thin films prepared at four different thicknesses is shown in Fig. 6. The direct band gap values are evaluated for $Cd_{0.3}Sn_{0.7}Se$ thin films having different thick-
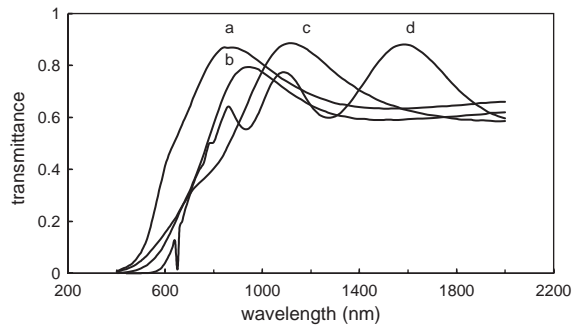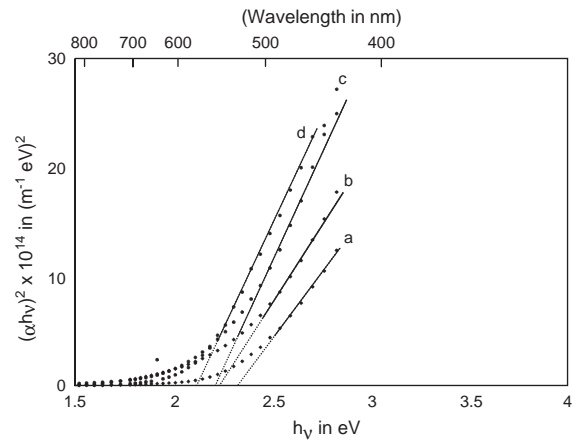
nesses of 0.225, 0.276, 0.3, and 0.683 μm and are listed in Table 3. It is observed that the band gap decreases with increase in the film thickness. Such a variation of band gap value with the film thickness has been reported by Shaalan and Müller [26] for their thermally evaporated cadmium selenide thin film and also by Pal et al. [30] for their vacuum evaporated polycrystalline cadmium selenide samples.

The transmission spectra for $Cd_{0.75}Sn_{0.25}Se$ thin films are shown in Fig. 7. The $(\alpha h\nu)^2$ versus $h\nu$ plot for $Cd_{0.75}Sn_{0.25}Se$ thin films is shown in Fig. 8. The increase in thickness of the film causes a shift of transmission spectrum towards higher

Table 3
Band gap energy and change in E_o of $Cd_xSn_{1-x}Se$ thin films with $x = 0, 0.3, 0.75$ and 1 prepared by vacuum deposition technique

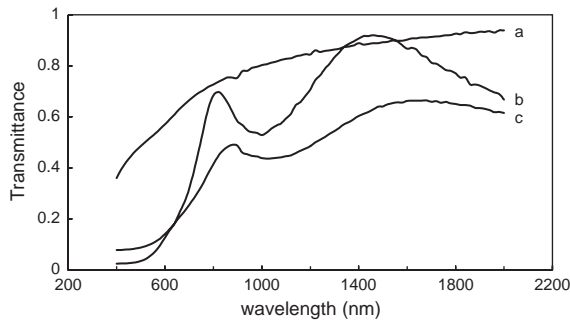| Thin film	Thickness (μm)	Band gap (eV)	E_o (eV)	ΔE (ev)
SnSe	0.2	1.26(4)	—	—
	0.2	1.23(3) (annealed at 300°C)		—
$Cd_{0.3}Sn_{0.7}Se$	0.225	2.17 (0.1)	2.055	0.226
	0.276	2.13 (0.1)		0.150
	0.300	2.11 (0.1)		0.110
	0.683	2.07(5)		0.030
$Cd_{0.75}Sn_{0.25}Se$	0.100	1.70 (5)	1.662	0.077
	0.168	1.68 (4)		0.041
	0.182	1.67 (8)		0.011
CdSe	0.343	E_{g1} 1.79(4)	1.660	0.261
		E_{g2} 1.98(1)		—
	0.403	E_{g1} 1.75(2)		0.173
		E_{g2} 1.99(2)		—
	0.497	**1.73 (2)**		0.133

Fig. 7. Transmittance spectra of $Cd_{0.75}Sn_{0.25}Se$ thin films prepared at room temperature and of thicknesses (a) 0.1 μm, (b) 0.168 μm and (c) 0.182 μm.

Fig. 8. A plot of $(\alpha h\nu)^2$ versus hν for $Cd_{0.75}Sn_{0.25}Se$ thin films prepared at room temperature and of thicknesses (a) 0.1 μm, (b) 0.168 μm and (c) 0.182 μm.

wavelengths. The band gap energies evaluated from the x-axis intercept are 1.70(5), 1.68(4) and 1.67(8) eV for the films of thicknesses 0.1, 0.168, and 0.182 μm, respectively and are displayed in Table 3.

3.3. Variation of band gaps with thickness

The variation of optical band gaps with thickness is analysed for CdSe, $Cd_{0.3}Sn_{0.7}Se$ and $Cd_{0.75}Sn_{0.25}Se$ thin films. In all the samples the band gap energy decreases with increase in thickness. A quantum size effect appears [10,31] in semiconductor and semimetal films when their
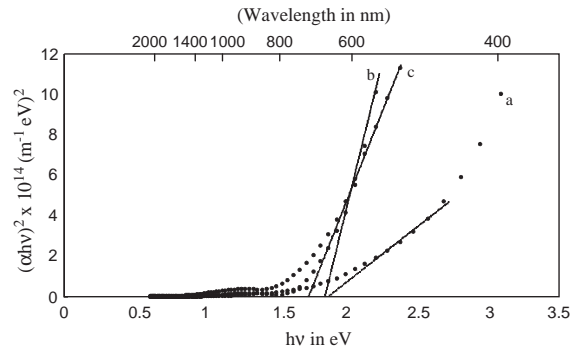
thickness is comparable with or smaller than both the mean free path and effective de Broglie wavelength of the carriers. Due to the finite thickness of the film, the electron energy states assume the discrete energy values in a thin film. Therefore, the conduction band and the valence band are separated by an additional amount of ΔE given by Bhatt et al. [10]

$$\Delta E \approx \frac{h^2}{8m^* t^2}, \qquad (4)$$

where t is the thickness and m^* is the effective carrier mass. From Eq. (4), ΔE is proportional to $1/t^2$ and hence a plot of band gap energy versus

$1/t^2$ will be linear. Plots between optical band gaps and $1/t^2$ for the CdSe, $Cd_{0.3}Sn_{0.7}Se$ and $Cd_{0.75}Sn_{0.25}Se$ thin films are shown in Fig. 9. Several workers [30,32] have obtained a similar variation in optical band gaps with thickness.

According to Damodara Das and Jagadeesh [25] a dislocation density of 10^{10}–10^{11} lines/cm^2 is frequently encountered in evaporated films. There are considerable lattice disturbances due to dislocations, namely, the local stress field around a dislocation, disrupted or dangling bonds with their specific charge and the space charge domain that form immediately in semiconductors. The compression and dilatation in stress patterns brought about by edge dislocations have an effect in changing the forbidden gap of the semiconductor. This is because of the result of local compression

Fig. 9. A plot of E_g versus $1/t^2$ for (a) CdSe, (b) $Cd_{0.3}Sn_{0.7}Se$ and (c) $Cd_{0.75}Sn_{0.25}Se$ thin films.

increment in the deformation–potential relation. Another influence is due to dangling bonds resulting in an energy level within the forbidden gap. If the distance between the individual sites of dislocation is larger than the lattice constants, alternate widening and narrowing of band gap occur. The original band gap 'E_o' would change by an additional amount ΔE because of isolated compression alone. Closely, superimposed dilatation would reduce this amount by $\Delta E'$ at the dilatation site. Since, $\Delta E' = \Delta E/2$, the resulting effective band gap is given by

$$E_{eff} = E_o + \Delta E/2. \tag{5}$$

Thus there is an overall increase in the forbidden gap of the evaporated thin films over that of their bulk values. In the case of CdSe thin films the band gap of the bulk sample is 1.7 eV. The band gap values obtained for CdSe thin films in the present studies are given in Table 3. The slight increase in the band gap values of CdSe thin films is due to the lattice disturbances and also due to the quantum size effect. For $Cd_{0.3}Sn_{0.7}Se$ and $Cd_{0.75}Sn_{0.25}Se$ thin films, no earlier reported values of bulk samples are available for comparison. However, the extrapolation of Fig. 9 to $x = 0$, gives the values of E_o for CdSe, $Cd_{0.3}Sn_{0.7}Se$ and $Cd_{0.75}Sn_{0.25}Se$ materials. Substituting the value of E_o in Eq. (5), the change in band gap energy, ΔE, for the above thin films are evaluated and are given in Table 3. It is evident from Table 3 that E_o value increases with increase in tin concentration in $Cd_xSn_{1-x}Se$ thin films.

3.4. Determination of grain size from band gap energy

The shift of optical band gap to higher value compared to its single crystal value is attributed to very small grain size of 3–10 nm and the resulting quantum confinement of electronic states in the thin films. For average grain radius [33],

$$E_g(R) \approx E_g(cryst) + \tfrac{1}{2}[(h^2/4)(m_e^{-1} + m_h^{-1})R^{-2}] - 1.8e^2/\varepsilon R, \tag{6}$$

where h is the Planck's constant, m_e and m_h are the effective masses of electrons and holes respectively,
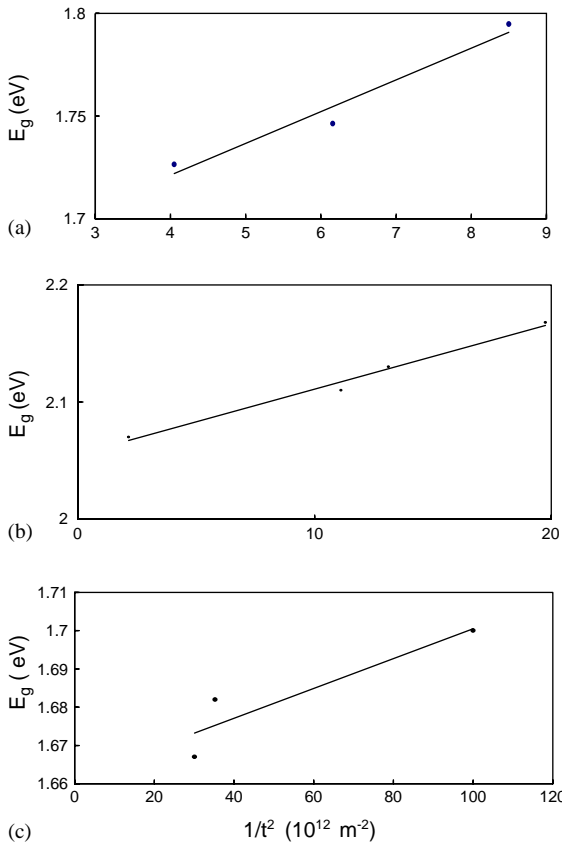
e is the electronic charge, and ε is the effective permittivity of the semiconductor expressing the shielding of the electron–hole Coulomb attraction. For smaller grain size, the R^{-2} term always dominates, shifting the band gap of the polycrystalline films towards higher value. From the above relation, it is clear that the increase of the grain size ($2R$) decreases the energy gap of the materials, whereas the decrease of the thickness increases the band gap. The grain sizes obtained for CdSe thin films using Eq. (6) are 4.12, 4.33, and 4.44 nm, respectively for the 0.343, 0.403, and 0.497 μm thick films. The values of $m_e = 0.13 \, m_o$, $m_h = 0.45 \, m_o$ and $\varepsilon = 8.85 \times 10^{-11} \, F/m$ for CdSe material are taken from standard tables [34]. The grain size calculated from XRD measurements for CdSe thin films, of thicknesses 0.343, 0.403, and 0.497 μm prepared at room temperature, for (0 0 2) peaks are 3.46, 3.48, and 3.51 nm, respectively. Single crystal band gap energy is not available for $Cd_{0.3}Sn_{0.7}Se$ and $Cd_{0.75}Sn_{0.25}Se$ in the literature for comparison. However, the observed band gap energy for $Cd_{0.3}Sn_{0.7}Se$ and $Cd_{0.75}Sn_{0.25}Se$ thin films is greater than their end members, CdSe and SnSe single crystals.

4. Conclusion

Optical properties of vacuum deposited $Cd_xSn_{1-x}Se$ thin films with $x = 0, 0.3, 0.75$ and 1 have been studied. The optical band gap energy is evaluated for various compositions and thicknesses. The studies reveal that these materials have a direct band gap energy and indirect band gap is improbable. The band gap variation for SnSe thin films due to annealing is very small. It indicates that there is a small increase in grain size of SnSe thin films because of annealing. The as deposited $Cd_{0.3}Sn_{0.7}Se$ thin films prepared at different thicknesses show no considerable variation in the optical band gaps indicating that the crystallinity does not considerably change with thickness in the range 0.225–0.683 μm. The band gaps variation in the as deposited $Cd_{0.75}Sn_{0.25}Se$ and CdSe thin films prepared at different thicknesses is likely to be attributed to an increase in particle size. The decrease in optical band gap energy with increase

in film thickness in these thin films is explained on the basis of quantum size effect. The band gap energy E_o increases with increase in concentration of tin in these films.

Acknowledgement

References

[1] C.R. Baxter, W.D. McLennan, J. Vac. Sci. Technol. 12 (1975) 110.
[2] W. Spachmann, E. Luder, T. Kalfab, W. Otterbach, Polycrystalline Semiconductors, Grain Boundaries and Interfaces, Springer, Berlin, 1989, p. 262.
[3] A. Van Calster, A. Vervaet, I. De Rycke, J. De Baets, J. Vanfleteren, J. Cryst. Growth 86 (1988) 924.
[4] M. Roth, Nucl. Instrum. Methods A283 (1989) 291.
[5] A. Burger, M. Roth, J. Cryst. Growth 67 (1984) 507.
[6] U. Pal, D. Samanta, S. Ghorai, B.K. Samantaray, A.K. Chaudhuri, J. Phys. D 25 (1992) 1488.
[7] .O.P. Agnihotri, A.K. Jain, B.K. Gupta, J. Cryst. Growth 46 (1979) 491.
[8] T. Terada, J. Phys. D 4 (1971) 1991.
[9] David R. Lide, H.P.R. Frederikse (Eds.), CRC Handbook of Chemistry and Physics, 75th ed, CRC Press Inc., USA, 1994, pp. 12–95.
[10] V.P. Bhatt, K. Gireesan, C.F. Desai, Cryst. Res. Technol. 24 (1989) 187.
[11] D. Louër, M. Louër, J. Appl. Crystallogr. 5 (1972) 271.
[12] A. Boultif, D. Louër, J. Appl. Crystallogr. 24 (1991) 987.
[13] B.D. Cullity, Elements of X-ray Diffraction, Addison-Wesley Publishing Co., Reading, MA, 1978, p. 324.
[14] T.J.B. Holland, S.A.T. Redfern, Mineralog. Mag 61 (1997) 65.
[15] D. Pathinettam Padiyan, A. Marikani, Cryst. Res. Technol. 37 (2002) 1241.
[16] D.T. Quan, Phys. Stat. Sol. (a) 86 (1984) 421.
[17] R.A. Smith, Semiconductors, 1 ed, Cambridge University Press, Cambridge, 1959.
[18] J.P. Singh, R.K. Bedi, J. Appl. Phys. 68 (1990) 2776.
[19] K.J. John, B. Pradeep, E. Mathai, J. Mater. Sci. 29 (1994) 1581.
[20] D. Pathinettam Padiyan, A. Marikani, K.R. Murali, Cryst. Res. Technol. 35 (2000) 949.
[21] M.T.S. Nair, P.K. Nair, R.A. Zingaro, E.A. Meyers, J. Appl. Phys. 74 (3) (1993) 1879.
[22] V.P. Bhatt, K. Gireesan, C.F. Desai, Cryst. Res. Technol. 25 (1990) 209.
[23] P.J. George, A. Sánchez, P.K. Nair, M.T.S. Nair, Appl. Phys. Lett. 66 (26) (1995) 3624.

[24] J.C. Slater, Phys. Rev. 103 (1956) 1631.

[25] V. Damodara Das, M.S. Jagadeesh, Mater. Res. Bull. 16 (1981) 1547.

[26] M.S. Shaalan, R. Müller, Sol. Cells 28 (1990) 185.

[27] G.K.M. Thutupalli, S.G. Tomlin, J. Phys. D 9 (1976) 1639.

[28] M. Cardona, K.L. Shaklee, F.H. Pollack, Phys. Rev. 154 (1967) 696.

[30] U. Pal, D. Samanta, S. Ghorai, A.K. Chaudhuri, J. Appl. Phys. 74 (10) (1993) 6368.

[31] K.L. Chopra, Thin Film Phenomena, New York, 1969.

[32] D. Samanta, B. Samanta, A.K. Chaudhuri, S. Ghorai, U. Pal, Semicond. Sci. Technol. 11 (1996) 548.

[33] M. Moskovits, in: G. Soles (Ed.), Chemical Physics of Atomic and Molecular Clusters, North-Holland, Amsterdam, 1990, p. 397.

[34] S.M. Sze, Physics of Semiconductor Devices, Wiley, New York, 1981, p. 848.